

## Supplementary Information for “Optimal quantum control using randomized benchmarking”

J. Kelly,<sup>1,\*</sup> R. Barends,<sup>1,\*</sup> B. Campbell,<sup>1</sup> Y. Chen,<sup>1</sup> Z. Chen,<sup>1</sup> B. Chiaro,<sup>1</sup> A. Dunsworth,<sup>1</sup> A. G. Fowler,<sup>1,2</sup> I.-C. Hoi,<sup>1</sup> E. Jeffrey,<sup>1</sup> A. Megrant,<sup>1</sup> J. Mutus,<sup>1</sup> C. Neill,<sup>1</sup> P.J.J. O’Malley,<sup>1</sup> C. Quintana,<sup>1</sup> P. Roushan,<sup>1</sup> D. Sank,<sup>1</sup> A. Vainsencher,<sup>1</sup> J. Wenner,<sup>1</sup> T. C. White,<sup>1</sup> A. N. Cleland,<sup>1</sup> and John M. Martinis<sup>1</sup>

<sup>1</sup>Department of Physics, University of California, Santa Barbara, CA 93106, USA

<sup>2</sup>Centre for Quantum Computation and Communication Technology,  
School of Physics, The University of Melbourne, Victoria 3010, Australia

### SCALING OF THE SENSITIVITY OF ORBIT WITH ERROR

Here, we derive the sensitivity of the sequence fidelity to gate error, and show that the sensitivity to fractional error is constant – hence ORBIT can in principle scale to arbitrarily small errors.

The sequence fidelity decays with  $m$  following  $F = Ap^m + B$ . For the single-qubit case:  $p = 1 - 2r$ , with  $r$  the error per Clifford. The variation in sequence fidelity with gate error is then

$$dF/dr = -2Am(1 - 2r)^{m-1}. \quad (S1)$$

The optimal value of  $m$  to operate ORBIT is at the characteristic decay of the sequence fidelity

$$m' = -1/\ln(1 - 2r) \quad (S2)$$

(this becomes clear when expressing the sequence fidelity as  $F = A \exp(-m/m') + B$ ). To quantify the scaling of the sensitivity with gate error, we evaluate the sensitivity at  $m'$ , where  $dF/dr$  is maximal.

$$\left. \frac{dF}{dr} \right|_{m=m'} = \frac{2A}{e(1 - 2r) \ln(1 - 2r)} \approx -\frac{A}{er}, \quad (S3)$$

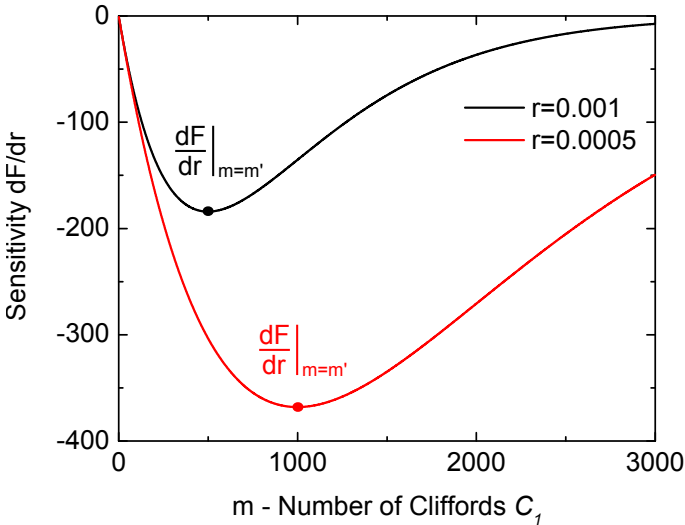


FIG. S1. The sensitivity of sequence fidelity to gate error (Eq. S1) for error per Clifford  $r = 0.001$  and  $r = 0.0005$ . We take the ideal value  $A = 0.5$  for the single-qubit case. Dots represent the optimal value of  $m = m'$  using Eq. S2 and Eq. S3.

with the right side an expansion for small  $r$ , keeping the lowest order term.

Importantly, the sensitivity to fractional error ( $dr/r$ ) is constant,

$$S = \frac{dF}{dr/r} = r \left. \frac{dF}{dr} \right|_{m=m'} \approx -\frac{A}{e}. \quad (S4)$$

This is a crucial result, as it implies that ORBIT scales to arbitrarily small error: the sensitivity is the same when improving the fidelity of a 99.0% gate to 99.9%, or a 99.99% gate to 99.999%; only the choice for  $m$  is different.

As an example, Eq. S1 is plotted in Fig. S1 for two cases:  $r = 0.001$  and  $0.0005$  ( $A = 0.5$ ). These cases reach a maximum sensitivity at  $m' = 500$  and  $m' = 1000$  respectively. When halving the error the optimal  $m$  and sensitivity double, as expected. We note that the sensitivity is retained for a wide range of  $m$  around the optimum, therefore the choice of  $m$  need not be exact. This is useful for improving gates, as we generally operate at a fixed  $m$ , and changes in  $r$  will affect  $m'$ .

### DEVICE PARAMETERS

qubits	Q <sub>0</sub>	Q <sub>1</sub>	Q <sub>2</sub>	Q <sub>3</sub>	Q <sub>4</sub>
$f_{10}$ (GHz)	5.805	5.238	5.780	5.060	5.696
nonlinearity (GHz)	-0.217	-0.226	-0.214	-0.212	-0.223

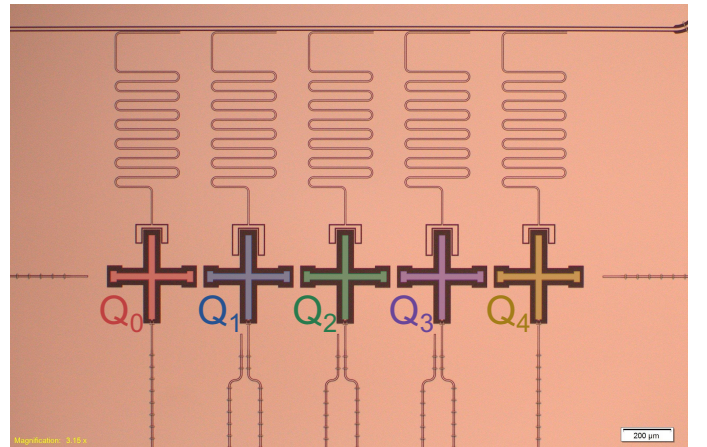


FIG. S2. Optical micrograph of the 5 Xmon transmon device. Qubits have individual XY and Z control with individual readout. Neighboring qubits have direct capacitive coupling of  $g/2\pi = 30$  MHz.

Additional information, including coherence times and fabrication details can be found in the Supplementary Information of Ref [1].

## EXPERIMENTAL SETUP

The wiring diagram and circuit components are shown in Fig. S4, reproduced from Ref [1].

### Electronics noise and drift

We find that electronics noise have a negligible effect on qubit control. We measure an output noise temperature of  $5 \cdot 10^3$  K from the room temperature electronics for the XY qubit control. There are two mechanisms that mitigate this noise: in-line attenuation and on-chip isolation. We have 40 dB in-line attenuation, and approximately 10 dB from cabling. The on-chip isolation is set by the coupling capacitance from the XY drive line to the qubit, which is approximately 60 aF [2]. We model the circuit as a  $50 \Omega$  line capacitively coupled to a qubit of characteristic impedance  $Z_q$ , as in Fig. S3. The isolation  $\Lambda$  is

$$\Lambda = \frac{V_1^2/Z_0}{V_2^2/Z_q} \quad (\text{S5})$$

$$= \frac{Z_0 Z_q}{(Z_c + Z_q)^2} \quad (\text{S6})$$

Using  $Z_0 = 50 \Omega$ ,  $Z_q = 300 \Omega$ ,  $Z_c = 1/i\omega C$ ,  $C = 60$  aF and  $\omega = 2\pi \cdot 6$  GHz and inserting into Eq. S6 we get  $\Lambda = 71$  dB isolation. This gives us a total of 121 dB attenuation, making the control electronics noise a negligible effect compared to the temperature of the environment.

We also must consider the noise coming from the Z control board. This will cause a jitter in the qubit frequency and manifest as dephasing. We find no difference in dephasing times when the Z control board is connected to the qubit or not, indicating this is not a limiting mechanism.

Lastly, we find that fidelities of the single- and two-qubit gates remain stable over the course of many hours from calibration, indicating that drifts in optimal parameters are small.

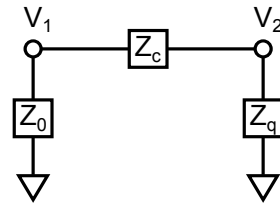


FIG. S3. Circuit model for qubit coupled to XY drive. Node 1 represents the XY drive line with impedance  $Z_0$ , which is capacitively coupled via  $Z_c$  to node 2 (the qubit) with characteristic impedance  $Z_q$ .

### CZ GATE FIDELITY BEFORE AND AFTER NELDER-MEAD OPTIMIZATION

The reference and interleaved randomized benchmarking data for the CZ gate, for Fig. 2 in the main text, are shown in Fig. S5. Figure S5a is before improvement, Fig. S5b after. The extracted fidelity of 0.993 is slightly lower than the extracted fidelity of 0.994 for the same pair of qubits in Ref. [1]. We attribute this to a small increase in the dephasing rate after thermally cycling the sample between experiments.

As a self-consistency check, we can calculate the expected error per Clifford using the derivation in Ref. [1]. We assume that gate errors are small and uncorrelated, such that adding errors is a good approximation. The expected error per Clifford is  $r_{\text{ref,predicted}} = 8.25 r_{\text{SQ}} + 1.5 r_{\text{CZ}}$  with  $r_{\text{SQ}}$  the average single-qubit gate error and  $r_{\text{CZ}}$  the CZ gate error. Assuming  $r_{\text{SQ}} = 0.001$ , we compute  $r_{\text{ref,predicted,before}} = 0.0318$  and  $r_{\text{ref,predicted,after}} = 0.0185$  which are close to the experimental values of  $r_{\text{ref,before}} = 0.0361$  and  $r_{\text{ref,after}} = 0.0188$ .

### CONTROL CROSSTALK DATA

The sequence fidelity data, for Fig. 4 in the main text, are shown in Fig. S6.

\* These authors contributed equally to this work

- [1] R. Barends, J. Kelly, A. Megrant, A. Veitia, D. Sank, E. Jeffrey, T. White, J. Mutus, A. Fowler, B. Campbell, et al., *Nature* **508**, 500 (2014).
- [2] R. Barends, J. Kelly, A. Megrant, D. Sank, E. Jeffrey, Y. Chen, Y. Yin, B. Chiaro, J. Mutus, C. Neill, et al., *Phys. Rev. Lett.* **111**, 080502 (2013).
- [3] J. Mutus, T. White, R. Barends, Y. Chen, Z. Chen, B. Chiaro, A. Dunsworth, E. Jeffrey, J. Kelly, A. Megrant, et al., arXiv preprint arXiv:1401.3799 (2014).

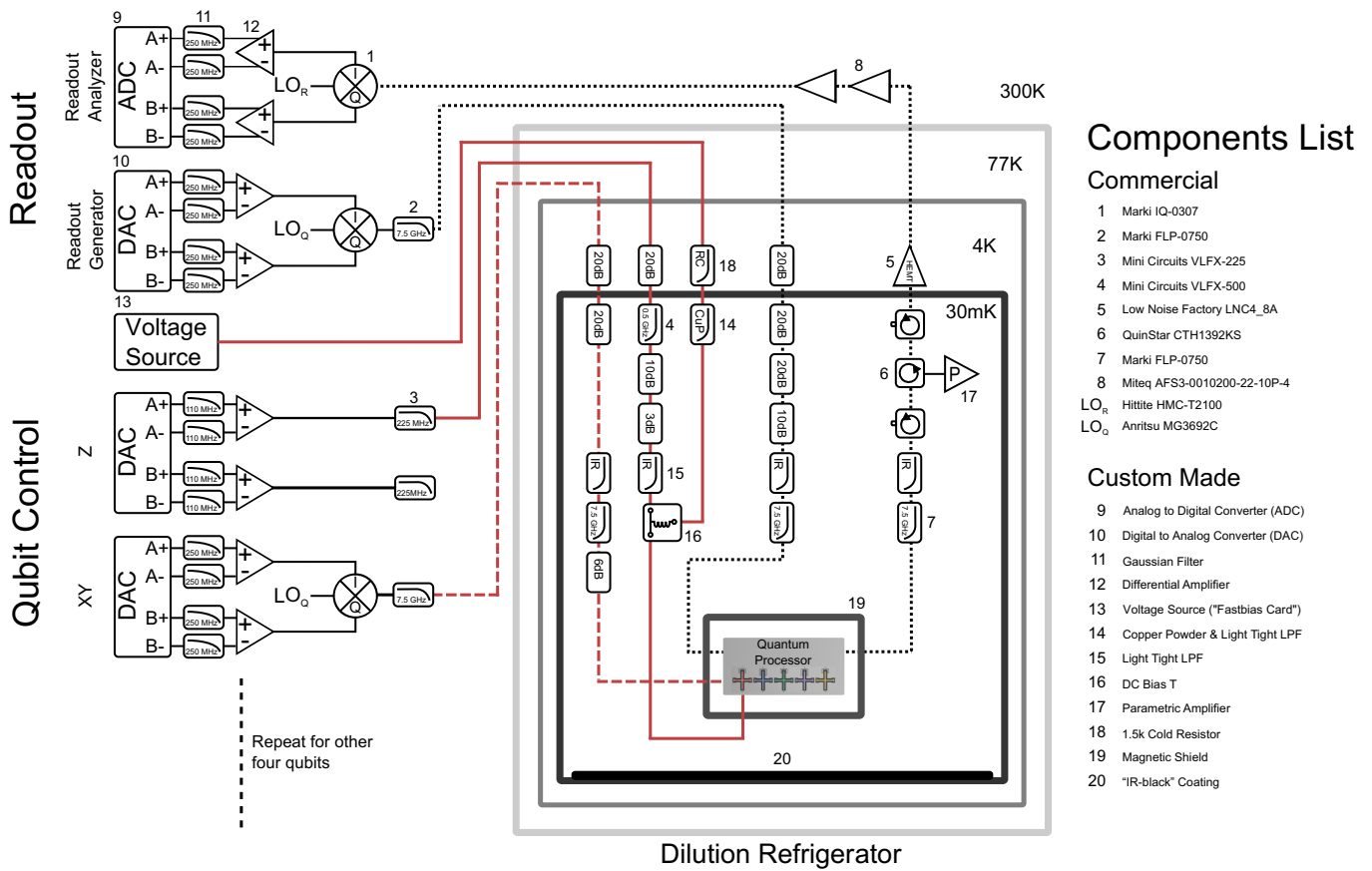


FIG. S4. (This figure reproduced from the Supplementary Information of Ref [1]) Electronics and Control Wiring. Diagram detailing all of the control electronics, control wiring, and filtering for the experimental setup. Each qubit uses one digital to analog converter (DAC) channel for each of the X, Y, and Z rotations. Additionally, we use a DC bias tee to connect a voltage source to each qubit frequency control line to give a static frequency offset. All five qubits are read out using frequency-domain multiplexing on a single measurement line. The readout DAC generates five measurement tones at the distinct frequencies corresponding to each qubit's readout resonator. The signal is amplified by a wideband parametric amplifier [3], a high electron mobility transistor (HEMT), and room temperature amplifiers before demodulation and state discrimination by the analog to digital converter (ADC). All control wires go through various stages of attenuation and filtering to prevent unwanted signals from disturbing the quantum processor. Two local oscillators ( $LO_Q$ ) are used for qubit XY control, at 4.5 and 5.6 GHz. The readout  $LO_R$  is at 6.76 GHz. All LO, DAC, and ADC electronics are locked to a 10 MHz SRS FS725 rubidium frequency standard.

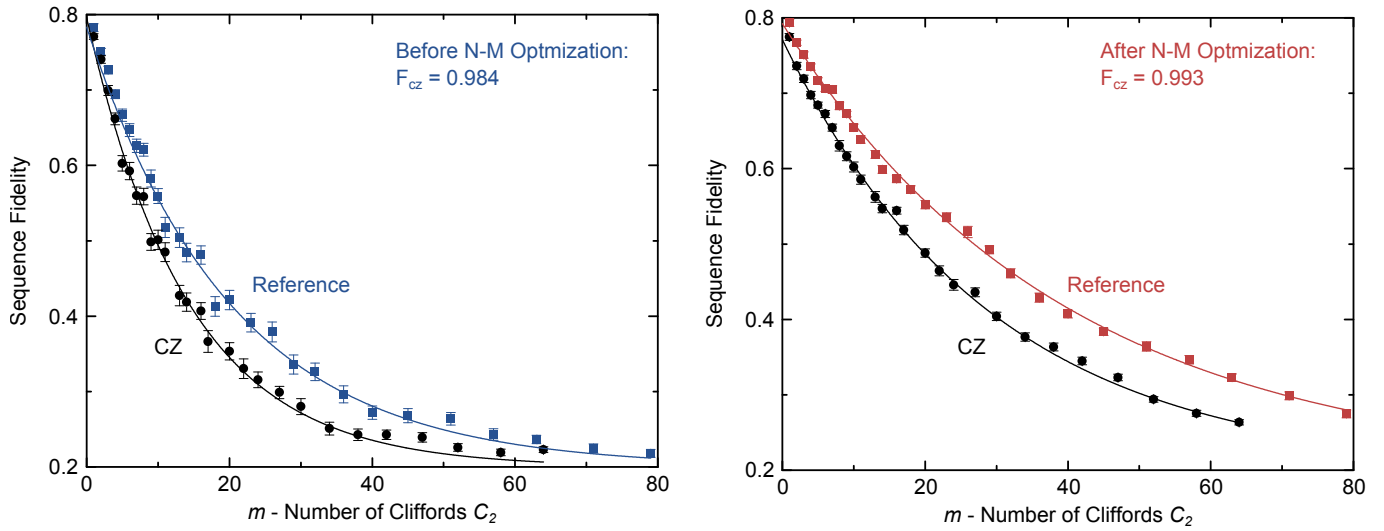


FIG. S5. Two-qubit randomized benchmarking data for Fig. 2 in the main text, showing the decay of the sequence fidelity of the reference and when interleaved with the CZ gate ( $k = 50$ ). (a) Before Nelder-Mead optimization. Reference error:  $r_{\text{ref}} = 0.0361$ , interleaved error:  $r_{\text{ref}+\text{CZ}} = 0.0511$ , extracted CZ error:  $r_{\text{CZ}} = 0.0157$ . (b) After Nelder-Mead optimization. Reference error:  $r_{\text{ref}} = 0.0188$ , interleaved error:  $r_{\text{ref}+\text{CZ}} = 0.0254$ , extracted CZ error:  $r_{\text{CZ}} = 0.0068$ .

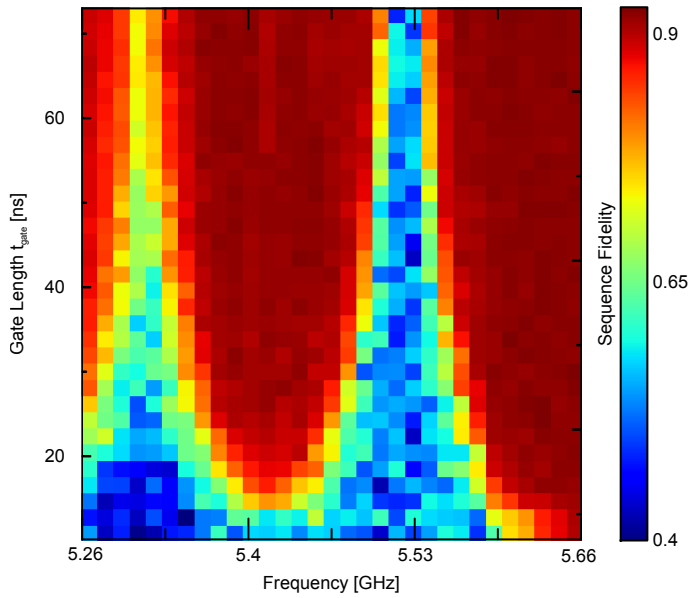


FIG. S6. Sequence fidelity data for Fig. 4 in the main text at  $m = 35$  ( $k = 20$ ).